

1.3 THE DETECTION OF π^0 MESONS, NEUTRONS AND NEUTRINOS AT THE 300 GeV ACCELERATOR

H. Leutz

CERN.

I. Introduction

The proposed large European accelerator is designed to accelerate every 3 sec about 3×10^{13} protons up to an energy of 300 GeV. Vague information only exists about types and dimensions of particle detectors to be used at this machine. Surveying existing devices which are suitable for the display of particle tracks and which could probably be useful in connection with the large accelerator we find:

- Spark- and wire chambers
- Heavy liquid bubble chambers
- Cryogenic bubble chambers.

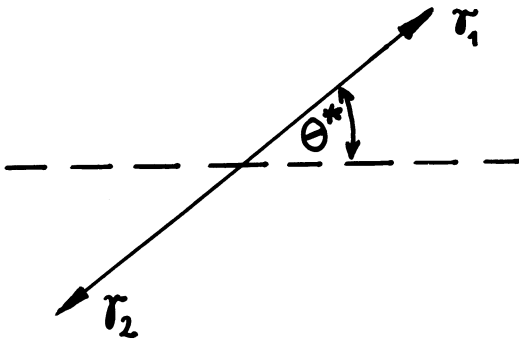
Since with the 300 GeV accelerator we aim at particle interactions producing rather high momentum transfers the number of neutral secondaries increases considerably as compared with present-day experiments. This is illustrated in fig. 1 which shows an extrapolation of the neutral fraction from the values established by recent experiments^{1,2,3,4,5)} to figures expected for higher CM - momenta. To yield unambiguous fits for the particle interactions produced at the 300 GeV accelerator it will be essential to identify π^0 -mesons and neutrons. Also reactions involving neutrinos and antineutrinos will play a vital part at the 300 GeV accelerator. Reasonable neutrino event statistics and complete neutrino event analysis are therefore essential and require adequate neutrino detection efficiency.

II. π^0 - Detection

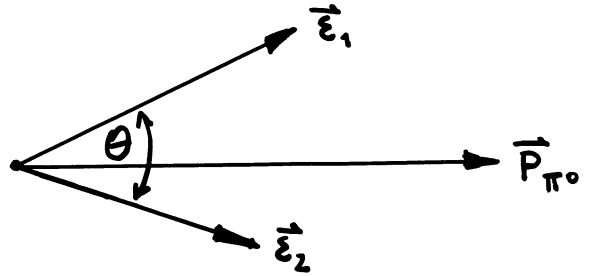
II.1 π^0 -Momentum Measurement

π^0 -Mesons decay after a mean lifetime of 0.9×10^{-16} sec into two γ -quanta with the energies ϵ_1 and ϵ_2 and the momenta $\vec{\epsilon}_1$ and $\vec{\epsilon}_2$, resp. Applying energy and momentum conservation we obtain:

CM - system



Lab - system



Energy conservation: $\epsilon_{\pi^0} = \epsilon_1 + \epsilon_2$
 Momentum conservation: $\vec{P}_{\pi^0} = \vec{\epsilon}_1 + \vec{\epsilon}_2$

$$\frac{m_{\pi^0}}{2 \sin \theta/2} = \sqrt{\epsilon_1 \epsilon_2} \quad (1)$$

The π^0 - momentum is determined by the two γ -directions (opening angle θ in the Lab-system) and by one γ -energy (ϵ_1 or ϵ_2) since the π^0 - rest mass m_{π^0} is known. Similar but more complicated relations⁶⁾ hold for the cases of two and three π^0 -mesons emerging from a particle reaction. In general we can state that knowledge of all γ -directions and of the energies from at least half the γ -quanta arising from π^0 -decays are necessary to determine the π^0 -momenta.

The consequences of this condition are demonstrated in fig. 2: The solid curves indicate the conversion probabilities for at least half the γ -quanta arising from one, two, and three π^0 -decays and

therefore stand for the efficiency of necessary γ -energy determinations. The dashed curves cover all γ -quanta of the corresponding decays and represent the efficiency of γ -direction determination. Based on fig. 2 we conclude that for an efficiency of 90% we need 1.5 radiation lengths for the γ -energies and about 5 radiation lengths for the γ -directions. This corresponds to the following layers of material:

- Spark- or wire chamber: 0.15 m (0.75 m) of aluminium divided into plates of adequate thickness.
- Propane chamber: 1.6 m (5.5 m) of propane.
- Cryogenic chamber: 15 m (50 m) of liquid hydrogen or 3.7 m (12.5 m) of 20 mol % Ne 80 mol % H₂-mixture.

By comparing the arrangement of conversion plates in spark- or wire chambers with the liquids in bubble chambers we find a significant difference: The accuracy of π^0 -momentum measurement increases with the number of conversion plates and with the distances between the plates so that the relative π^0 -momentum error is strongly connected with the space available for a spark- or wire chamber arrangement. Only in the extreme case where the plate arrangement has the same average density as liquid hydrogen do we obtain comparable π^0 -momentum accuracies but also comparable linear dimensions for both devices. However the production of Bremsstrahlung - quanta which considerably disturb the π^0 -identification would still be much higher in metal plates than in liquid hydrogen.

II.2 π^0 -Momentum Error

The relative π^0 -momentum errors $(\frac{\Delta p}{p})_{\pi^0}$ which can be expected for the different detectors can be roughly estimated from an error formula given by Trilling⁷:

$$\left(\frac{\Delta p}{p}\right)_{\pi^0} = \frac{\cos \theta^*}{\sqrt{\left(\frac{\xi_1}{\Delta \xi_1}\right)^2 + \left(\frac{\xi_2}{\Delta \xi_2}\right)^2}}$$

Using the relations

$$\frac{\Delta \xi_1}{\xi_1} = -\frac{\Delta \xi_2}{\xi_2} \quad \text{and} \quad \cos \theta^* = \frac{\xi_1 - \xi_2 + \sqrt{\Delta \xi_1^2 + \xi_2 \Delta \xi_2^2}}{P}$$

we finally obtain an error formula which of course does not include errors due to γ -direction determination:

$$\left(\frac{\Delta p}{p}\right)_{\pi^0} = \frac{1}{\sqrt{2}} \frac{\Delta \xi_1}{\xi_1} \left(\frac{\xi_1 - \xi_2}{P_{\pi^0}} + \frac{\Delta \xi_1}{\xi_1} \right) \quad (3)$$

Since the γ -energy ξ_1 will be measured via the momenta of the (e^+, e^-) - pair we obtain:

$$\frac{\Delta \xi_1}{\xi_1} = \sqrt{\left(\frac{\Delta e^-}{e^-}\right)^2 + \left(\frac{\Delta e^+}{e^+}\right)^2}$$

Now we make the following assumptions:

- The π^0 -momentum p_{π^0} is shared between the two γ -quanta in such a way that $(\xi_1 - \xi_2)/p_{\pi^0} = 0.5$; this corresponds to the statistical average for the distribution of the two γ -energies ξ_1 and ξ_2 (see relations (6) and (7)).
- The larger γ -energy ξ_1 is equally shared in the (e^+, e^-) -pair.

From these assumptions follows for the (e^+, e^-) -momenta e

$$e = 0.375 p_{\pi^0}$$

and relation (3) can be changed into:

$$\left(\frac{\Delta p}{p}\right)_{\pi^0} = \frac{\Delta e}{e} (0.5 + \sqrt{2} \frac{\Delta e}{e}) \quad (4)$$

⁺ including the errors for the γ -energies

The relative electron (positron) - momentum error $\frac{\Delta e}{e}$ is composed of the errors due to the measurement of track curvature in the magnetic field (M), multiple Coulomb scattering (s) and radiation loss (R):

$$\frac{\Delta e}{e} = \sqrt{M^2 + S^2 + R^2} \quad (5)$$

By minimizing the error given by relation (5) we obtain optimum track lengths for the (e^+, e^-) - pairs in the different liquids. Using these optimum track lengths we calculate the values for M, S, and R, obtain the relative pair momentum error $\frac{\Delta e}{e}$ and with relation (4) finally get the relative π^0 -momentum errors which are plotted for hydrogen, propane and a 20 mol % Ne - 80 mol % H_2 -mixture in fig. 3.

II.3 γ -Angular Distributions

In the CM - system we have the following simple relation between the γ -energies ξ_1^* , and ξ_2^* and the π^0 -rest mass:

$$\frac{m_{\pi^0}}{2} = \xi_1^* = \xi_2^*$$

Transformation into the Lab-system yields:

$$\begin{aligned} \xi_1 &= \frac{\xi_{\pi^0}}{2} + \frac{p_{\pi^0}}{2} \cos \theta^* \\ \xi_2 &= \frac{\xi_{\pi^0}}{2} - \frac{p_{\pi^0}}{2} \cos \theta^* \end{aligned}$$

$$\xi_1 - \xi_2 = p_{\pi^0} \cos \theta^* \quad (6)$$

By simple geometric considerations we evaluate the probability S for γ -emission into the angular interval between $\theta^* = 90^\circ$ (transversal π^0 -decay in the CM-system) and an angle θ^* :

$$S = \cos \theta^* \quad (7)$$

From relations (1), (6), and (7) we obtain for the opening angle θ between the two γ -directions in the Lab-system:

$$\sin \theta/2 = \frac{1}{\gamma} \frac{1}{\sqrt{1-\beta^2 S^2}} \quad (8)$$

γ = Lorentz factor (ratio of moving to rest mass of π^0)

β = relativistic π^0 -velocity

Based on relation (8) the distribution of opening angles θ for γ -quanta emitted from π^0 -decays is shown in fig.4. The minimum angle indicated in this figure corresponds to the case of transversal π^0 -decay in the CM - system (Lab-system: $\sin \theta \text{ min}/2 = 1/\gamma$). By multiplying the scale on the x-axis with the ratio of the corresponding Lorentz factors we obtain the θ -distribution for other π^0 -momenta.

To obtain the distribution of γ -directions in the Lab-system we also must take into account the π^0 -directions. For the CM-system the momentum distributions of π -mesons obtained from 17 GeV/c (π^- ,p) - interactions⁸⁾ have been extrapolated to 100 GeV/c by Fiorini⁹⁾. Transformation into the Lab-system yields the ($p_L - p_t$) - plot shown in fig. 5. Finally, we obtain the following rough estimate for the distribution of γ -quanta arising from π^0 -mesons produced at 100 GeV/c primary interactions:

Table 1

angular interval	0 - 10 mrad	10 - 175 mrad	10° - 30°	30°-60° 120°-150°	60° - 120°
relative γ -intensity	25%/o	40%/o	15%/o	8%/o	12%/o

III. Neutrons

Since neutrons are stable and neutral particles, they can be detected from interactions with other particles only. Best conditions to fix the neutron parameters are offered by hydrogen where the neutron momentum can be derived from the track of the recoil proton and from the neutron direction which is fixed by the two points of primary and secondary interactions. The efficiency of neutron identification is shown in fig. 6 for liquid hydrogen layers of 2 m (dashed curve) and 10 m (solid curve). The curve indicating elastic proton recoil peaks at about 0.3 GeV/c neutron momentum. The decrease at lower momenta results from unmeasurable recoil tracks. We assumed a minimal measurable track length of 2 mm. The inelastic cross section, which dominates above 1.5 GeV/c neutron momentum, still permits neutron identification but does not allow the measurement of neutron momenta.

Using again Fiorini's extrapolation to 100 GeV/c (π^- ,p) - interactions, the distribution of neutron momenta in the Lab-system is shown in fig. 7. Most neutron momenta are in a range where elastic proton recoil dominates and also most neutrons are emitted under rather large angles from the incident beam.

IV. Neutrinos

The proposed 300 GeV accelerator will, because of the proton energy and intensity envisaged, change the energy range and the intensity of future neutrino beams considerably. In general, there will be two possibilities to guide a neutrino beam into a detector:

- 1) Wide Band System (WBS): This is a scaled up version of the present CERN layout. The neutrino parents are guided by a weak focussing system (horn, reflectors etc), which yields rather high neutrino intensity but creates severe muon shielding

difficulties. The iron shield should have a length of 200 m and a weight of about 70 000 to.

- 2) Narrow Band System (NBS): The meson beam will be guided by quadrupoles of modest aperture towards the detector. Muons are deflected by a magnet at the end of the decay channel. This layout yields neutrino beams having a defined band width but less intensity than with the WBS.

Some preliminary data concerning the neutrino layout at the 300 GeV accelerator are listed in table 2. With respect to the detectors we distinguish two parameters which are essential for the neutrino efficiency:

- The NBS provides a pencil beam of neutrinos in the detector. Therefore the detector length only will be essential for the neutrino detection efficiency.
- The WBS produces a slightly diverging beam having a cross section diameter between 2 m and 3 m. For all detectors having a smaller cross section the neutrino detection efficiency then increases approximately with the product of detector length and the average linear dimension of the detector cross section, i.e. with the so called longitudinal cross section of the arrangement.

Based on these suggestions and on the data listed in table 2 a rough estimate for neutrino event rates at the 300 GeV accelerator in several bubble chambers is given in table 3.

V. Conclusions

V.1 Type of Detector

The advantages and drawbacks of different detector types cannot be judged with respect to the identification of neutral particles only. In comparing first spark - (wire) chambers and bubble chambers it is clear that both types must have a magnetic field which will be generated by superconducting coils. Including the necessary buildings the costs for both types will not differ very much at equal detector dimensions.

Spark- and wire chambers are biased by the necessary triggering system and therefore produce a rather large amount of preselected data. They are capable of operation online with an electronic computer and hence allow rapid data processing and therefore yield high event statistics. Bubble chambers record all the charged products of collisions in an unbiased way and the particle tracks are fully visible even in the immediate vicinity of the interaction. Therefore bubble chamber film stores a large quantity of information which must be selected and processed after the exposure. Although the two types of detectors should therefore be complementary at the 300 GeV accelerator we may state that for neutrino physics bubble chambers are indispensable.

In principle we distinguish two kinds of bubble chambers, the heavy liquid (propane, freon) chamber and the cryogenic (hydrogen/deuterium/neon) chamber. Due to the high density of the filling medium the heavy liquid chamber provides good γ -detection efficiency. The cryogenic chamber filled with liquid hydrogen provides free protons as target material or when filled with liquid deuterium offers the simplest available neutron target. With an addition of liquid neon to the liquid hydrogen¹⁰⁾ the cryogenic chamber covers with the different mixture ratios all radiation lengths from 10 m (pure hydrogen) down to 0.29 m (pure neon). By mounting a volume separated target, in which also tracks can be photographed in the cryogenic chamber¹¹⁾, it is even possible to have free protons (by filling the target with hydrogen) or quasi free neutrons (by filling the target with deuterium) for the primary interactions and a liquid of higher density (by filling the chamber with a hydrogen - neon mixture) to provide enough γ -detection efficiency.

It is evident that measurement of neutron momenta calls for hydrogen, and that neutrino events in hydrogen or deuterium can be best interpreted. Taking into account all the possibilities listed above

I conclude that a cryogenic bubble chamber should be available at the 300 GeV accelerator.

V.2 Dimension of Detector

The linear dimensions of an instrument necessary for the detection and measurement of neutrals are influenced by the following aspects:

- detection efficiency for γ -quanta, neutrons and neutrinos
- measuring accuracy for π^0 -mesons and neutrons.

As far as detection efficiency only is concerned a detector consisting of high density material reduces the linear dimensions and hence the price of the arrangement considerably as compared with hydrogen or deuterium. A propane chamber or a 50 mol % Ne - 50 mol % H₂ - chamber detects within 5 m about 90% of all γ -quanta arising from one, two and three π^0 -decays (see fig. 2). As already mentioned this advantage will be purchased by the drawbacks inherent in targets of complicated nuclear structure.

As expected, the π^0 -momentum errors, which are due to the measuring inaccuracies for (e^+ , e^-) - pairs, increase rather rapidly with decreasing radiation length of the chamber fluid (see fig. 3). The influence of magnetic field strength and of sagitta error on the π^0 -momentum error is less significant than that of the chamber fluid.

According to fig. 5 34% of all 10 GeV/c (100 GeV/c) π^0 -mesons emit their γ -quanta into the angular interval between 26 (2.6) mrad and 28 (2.8) mrad. It will therefore be very difficult to determine the γ -directions accurately from the spatial position of the conversion points. To obtain an accuracy comparable to or better than that expected for the measurement of (e^+ , e^-) - momenta we need on the average

at least 3 m distance between the π^0 -decay point and the γ -conversion points.

The most serious distortions for π^0 -measurement arise from radiative energy loss of (e^+, e^-) - pairs, because the Bremsstrahlung-quanta may simulate γ -quanta arising from π^0 -decay and hence prevent unambiguous correlation of the γ -pairs. Since the radiation loss rises as the square of the atomic number, the ratio of radiation loss to ionization loss (increasing with the atomic number only), from which the fraction of electron kinetic energy going into shower production can be evaluated, is smallest for hydrogen: $H_2 \sim 3$; Propane ~ 10 ; Al ~ 20 at 1 GeV/c electron momentum which corresponds on the average to 2.7 GeV/c π^0 -momentum.

Taking into account the above mentioned difficulties for π^0 -momentum measurements and including the arguments already discussed for neutron momentum measurement and neutrino physics it turns out that a cryogenic chamber offers the best adaptability at the 300 GeV accelerator. In this case we should aim at a linear dimension of about 15 m because of the following requirements:

- To get a 90% probability for the measurement of γ -energies necessary to determine π^0 -momenta (see fig.2) we need about 15 m of liquid hydrogen. The missing γ -directions can be determined from the conversions in a metal plate (thickness corresponding to 3.5 rad lengths) which is mounted near the chamber wall.
- If we operate a hydrogen (deuterium) target (diameter between 2 m and 3 m) in a cryogenic chamber filled with a mixture of 20 mol % Ne and 80 mol % H_2 we need about 12 m to convert 90% of all γ -quanta arising from π^0 -decays.
- In a chamber with 15 m linear dimension the requirements for the spatial resolution of γ -conversion points to get adequate accuracies for the γ -directions are fulfilled.

- The dimension required for neutron momentum measurement fits well into the proposed dimension of 15 m (see fig. 6).
- According to table 2 a linear dimension of 15 m yields already reasonable neutrino event rates even in the cases of neutrino beams having selected band widths.

V.3 Shape of Detector

Considering this question we must pay attention to the following aspects:

- Directions of produced neutral secondaries
- Directions of incoming beams
- Questions associated with optics and data handling
- Shape of superconducting coils
- Problems caused by filling a large chamber with deuterium.

Neutrons are mostly (see fig. 7) and γ -quanta rather frequently (see table 1) emitted into the angular interval between 30° and 90° from beam direction. According to preliminary studies of beam layouts¹²⁾ at the 300 GeV accelerator a large bubble chamber will be located at the cross point of various beams (neutrino beam, mass separated beams having design momenta of 150 GeV/c, 100 GeV/c, and 50 GeV/c). It would, therefore, be very inconvenient if the chamber, because of a longitudinal shape, were polarized towards one beam direction only. The preferable optical arrangement would be to photograph the volume of a rather flat cylindrical chamber with four or five cameras from bottom or top. This provides rather large volumes to be photographed by each camera and facilitates scanning and data handling. For reasons of technical feasibility the superconducting coils should be arranged so as to have circular windings and a vertical axis. In this case we have vertical magnetic field direction and hence no component of magnetic field acting on charged particles perpendicular to the horizontal symmetry plane of the chamber. Therefore the useful height of

the chamber could be limited to about 4 m. This restriction is also favourable for the optical path lengths which should be as short as possible to reduce optical distortions caused by thermal turbulences in the chamber liquid.

Considering the last point it is quite clear that a bubble chamber of the dimensions envisaged could hardly be filled with deuterium having a tritium contamination which is low enough for doing neutrino physics. To overcome this difficulty a mylar tube (15 m long and 2 m in diameter) should be filled with deuterium. The symmetry axis of this tube should coincide with the axis of the neutrino beam inside the chamber. In this arrangement we get a deuterium filled target for a neutron beam which should be surrounded by a mixture of hydrogen and neon. For the investigation of strong interactions the deuterium should be filled into a flat cylindrical target (2 m diameter, 30 cm high) having a vertical axis and mounted in the beam plane near the entrance window.

Summary

With respect to the detection of π^0 -mesons, neutrons and neutrinos the construction of a cylindrical shaped cryogenic bubble chamber with about 15 m diameter, a vertical symmetry axis and a useful height of about 4 m at the 300 GeV accelerator is proposed. Depending on the experiments envisaged this chamber could be filled with hydrogen or with neon-hydrogen mixtures. Beam targets made of mylar, filled with hydrogen or deuterium and having appropriate shapes for neutrino- or strong interaction physics, should be mounted inside this chamber. As a first approach to such an instrument D.B.Thomas will present a technical proposal for a Mammoth chamber in the course of this colloquium.

References:

- 1) Aachen-Berlin-CERN collaboration: private communication
- 2) Aachen-Birmingham-Bonn-Hamburg-London-München collaboration: private communication
- 3) F.E.James et al.: Phys.Rev. 142, 896 (1966)
- 4) P.Daronian et al.: Nuovo Cimento 41, 503 (1966)
- 5) C.A.Tilger et al.: Phys.Rev. 142, 972 (1966)
- 6) H.Leutz and G.Rau: CERN/TC/BEBC 65-3
- 7) G.Trilling: SLAC - Report No 5 (1962)
- 8) R.Huson and W.B.Tretter: Nuovo Cimento 33, 1 (1964)
- 9) E.Fiorini: CERN/ECFA 66/WG2/VS-SG3/EF1
- 10) R.C. Albert, C.L.Goodzeit, F.C.Pechar, and A.G.Prodell: Advances in Cryogenic Engineering
- 11) H.Leutz: CERN/TC/BEBC 66-21
- 12) ECFA Report 1967: CERN/ECFA 67/13/Rev.2 (layout for experimental area II)

Item	Dimensions	
Proton momentum	300 GeV/c	
Number of circulating protons	3×10^{13}	
Frequency of beam ejection	1 every 3 sec	
Target efficiency	50%	
Meson focussing system	WBS	NBS
Length of decay channel	500 m	700 m
Muon shielding	200 m Fe	magnet
Neutrino intensity: peaked at 8 GeV	$6.5 \times 10^{-3} \frac{\gamma}{m^2 p}$	
peaked at 20 GeV	$1.1 \times 10^{-3} \frac{\gamma}{m^2 p}$	
peaked at 40 GeV	$7.5 \times 10^{-5} \frac{\gamma}{m^2 p}$	
peaked at 100 GeV	$2.9 \times 10^{-5} \frac{\gamma}{m^2 p}$	
Gargamelle: length	4.4 m	
longitudinal cross-section	10 m ²	
3.5 m chamber: length	3.5 m	
longitudinal cross-section	7.8 m ²	
Mammoth chamber: length	15 m	
longitudinal cross-section	60 m ²	

Table 2: Preliminary data for neutrino layout at the 300 GeV accelerator

Reaction	ν - Beam		Gargamelle*			3.5 m - Chamber			Mammoth - Chamber		
	System	Energy	elastic	inelastic	total	elastic	inelastic	total	elastic	inelastic	total
$\bar{\nu}$ in H ₂	WBS	8	78	65	143	61	51	112	440	360	860
	NBS	20	16	13	29	10	8	18	42	35	77
	NBS	50	1.1	0.9	2	0.7	0.6	1.3	3.0	2.4	5.4
	NBS	100	0.4	0.3	0.7	0.25	0.2	0.45	1.1	0.9	2.0
ν in D ₂	WBS	8	360	690	1050	280	530	810	2000	3900	6000
	NBS	20	75	140	215	47	90	137	200	380	580
	NBS	50	5.2	10	15.2	3.2	6.1	9.3	14	25	40
	NBS	100	2.0	3.8	5.8	1.2	2.3	3.4	5	9	14

* Neutrino event rates on H - (D) - atoms in propane (deuterized propane) only

Table 3: Estimate of neutrino event rates per day at 300 GeV accelerator

π^+ LAB - MOMENTUM [GeV/c]

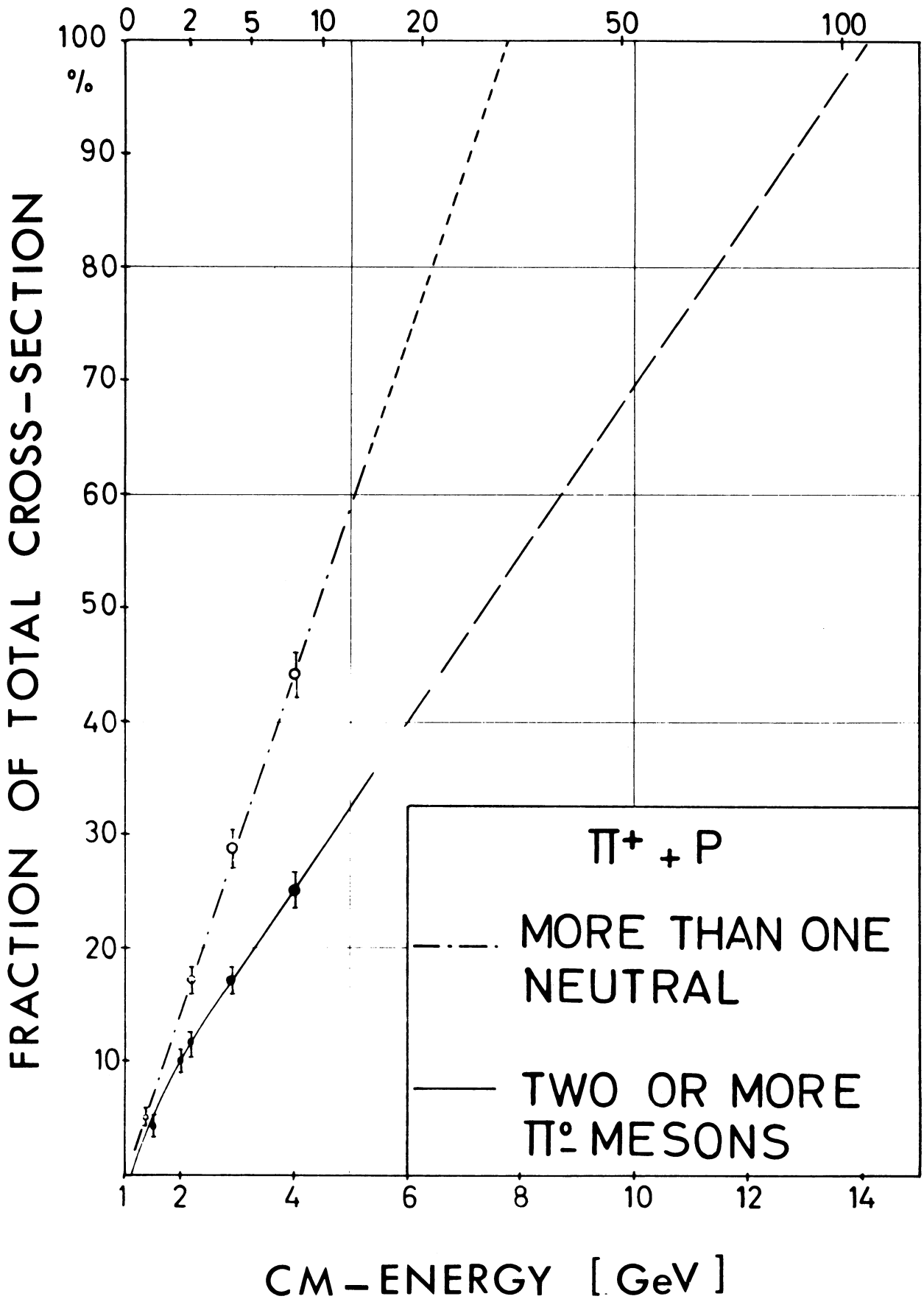
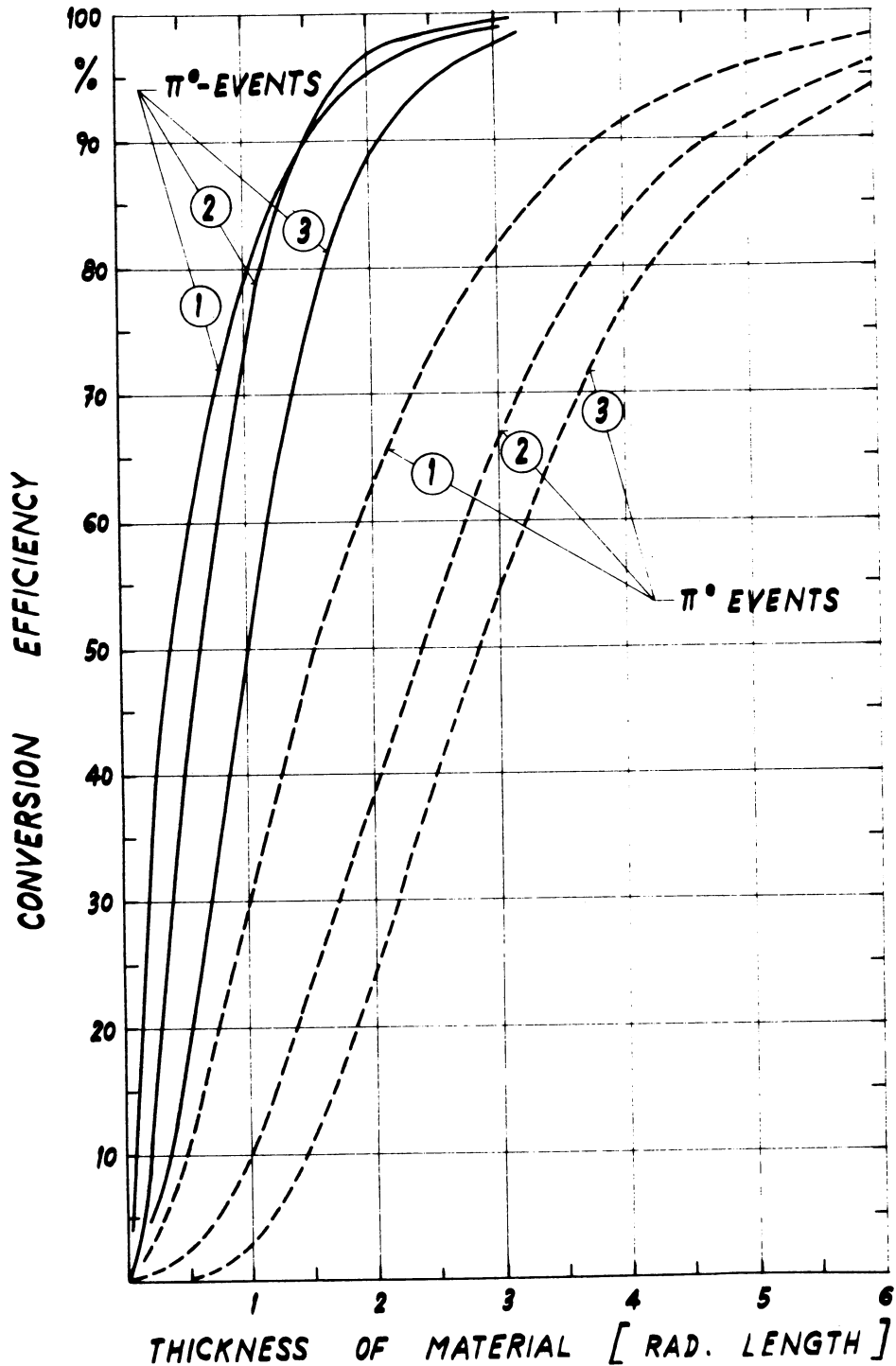


Fig. 1: Increase of neutral fraction with CM - energy



	————— Energy	----- Direction	
One π^0 - Event:	$2q - q^2$	q^2	$q = \gamma$ -conversion probability
Two π^0 - Events:	$(2q - q^2)^2$	q^4	
Three π^0 - Events:	$(2q - q^2)^3$	q^6	

Fig. 2:

Conversion efficiency for at least one, two or three γ -quanta arising from one, two or three π^0 -decays, resp. (solid curves). These are the conversion efficiencies required for γ -energy determination. The dashed curves refer to the conversion efficiency for all γ -quanta produced in one, two or three π^0 -decays: γ -direction determination.

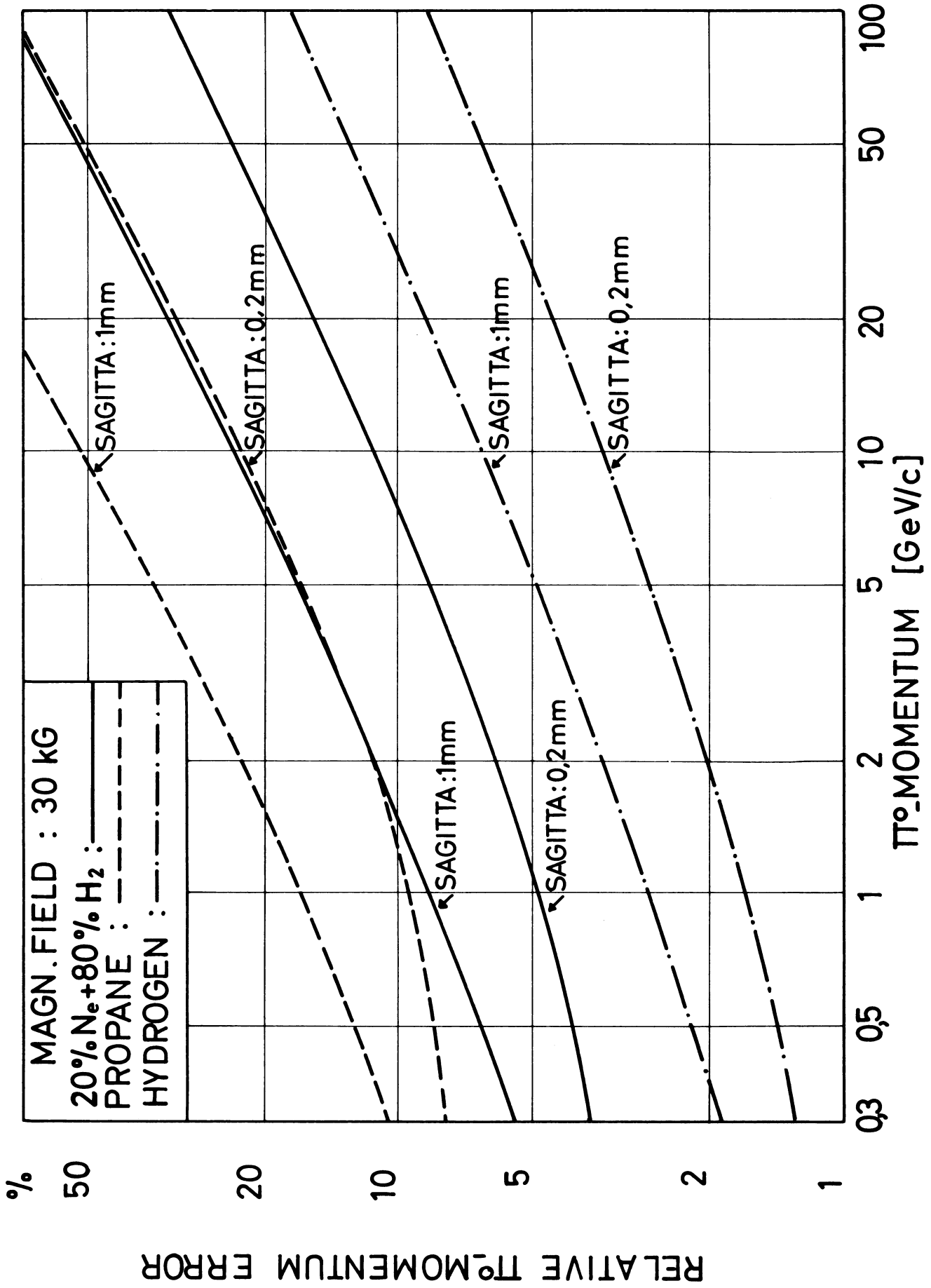


Fig. 3: Relative π^0 - momentum error in different chamber liquids.

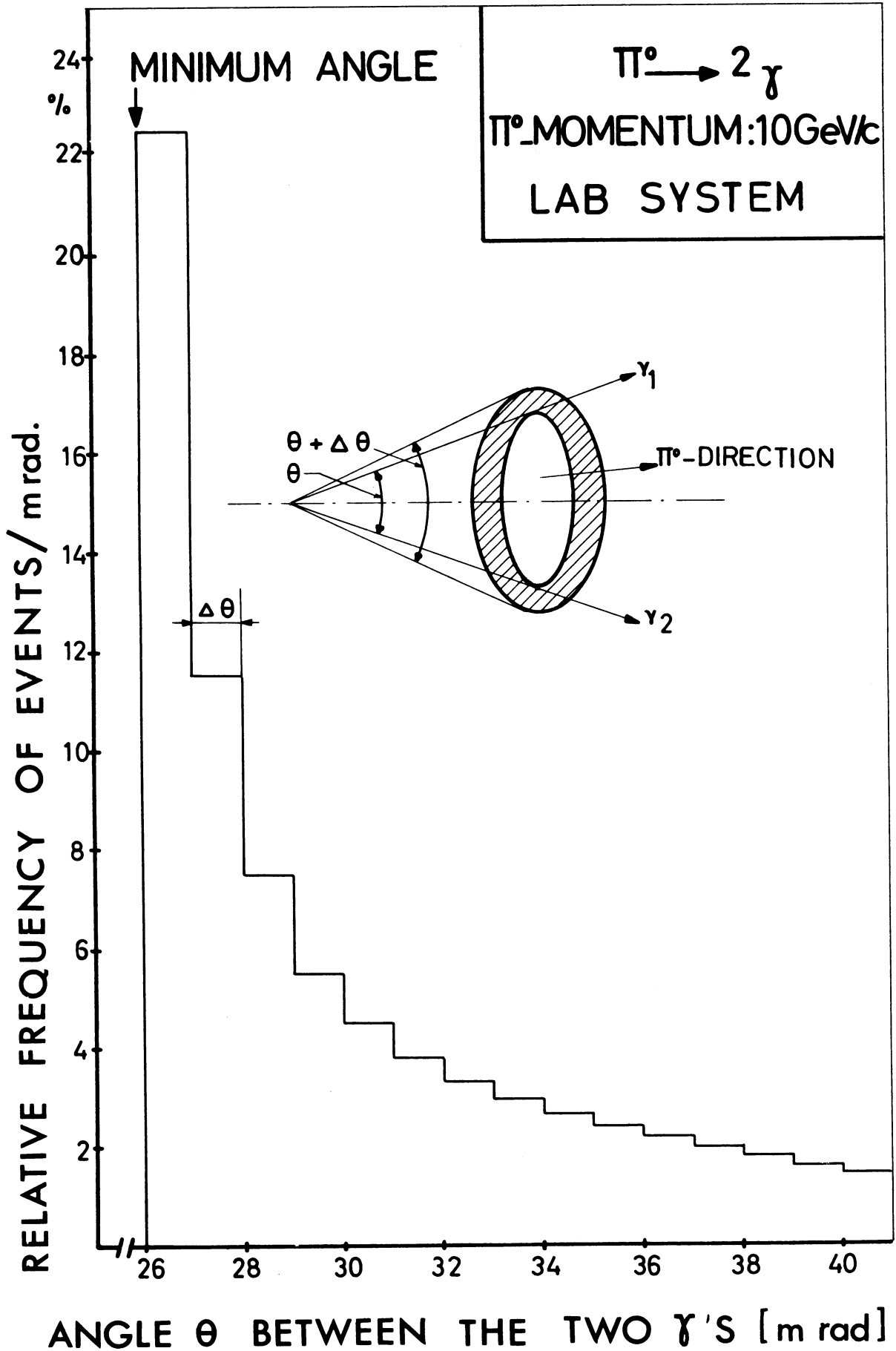


FIG:4

LAB - SYSTEM

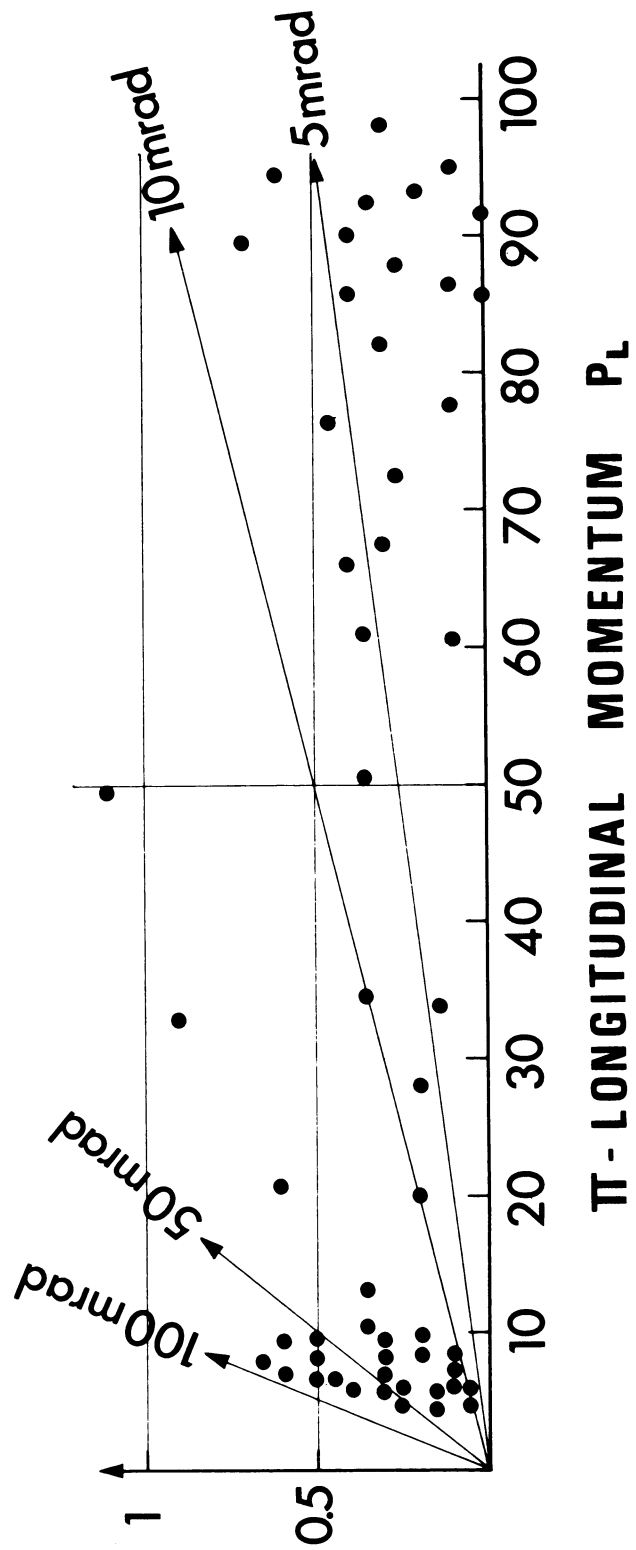
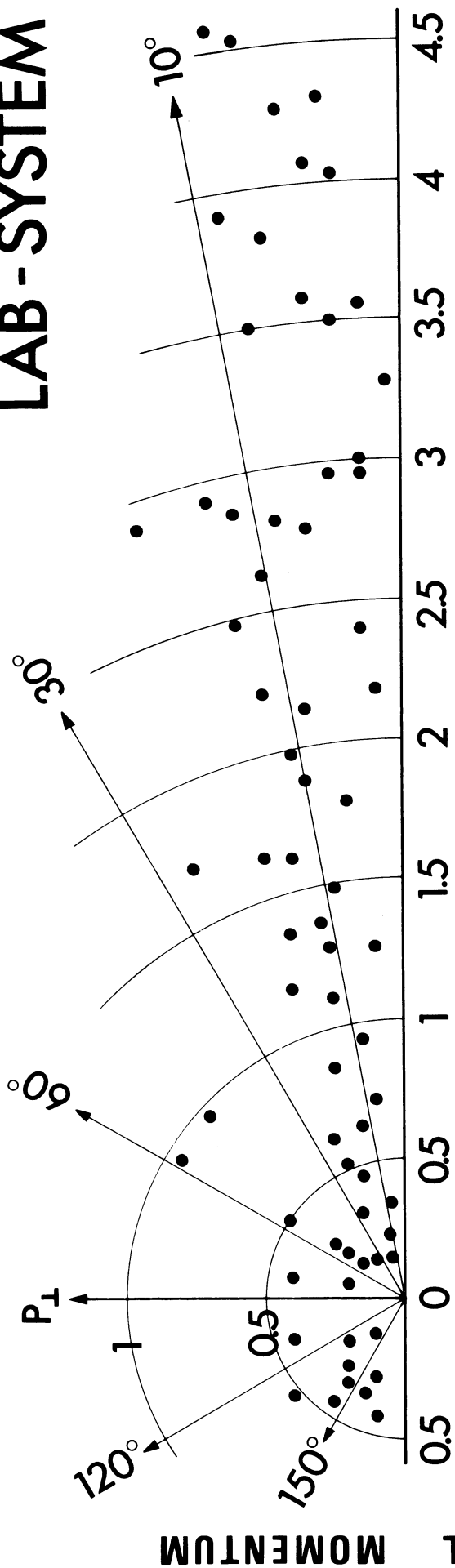
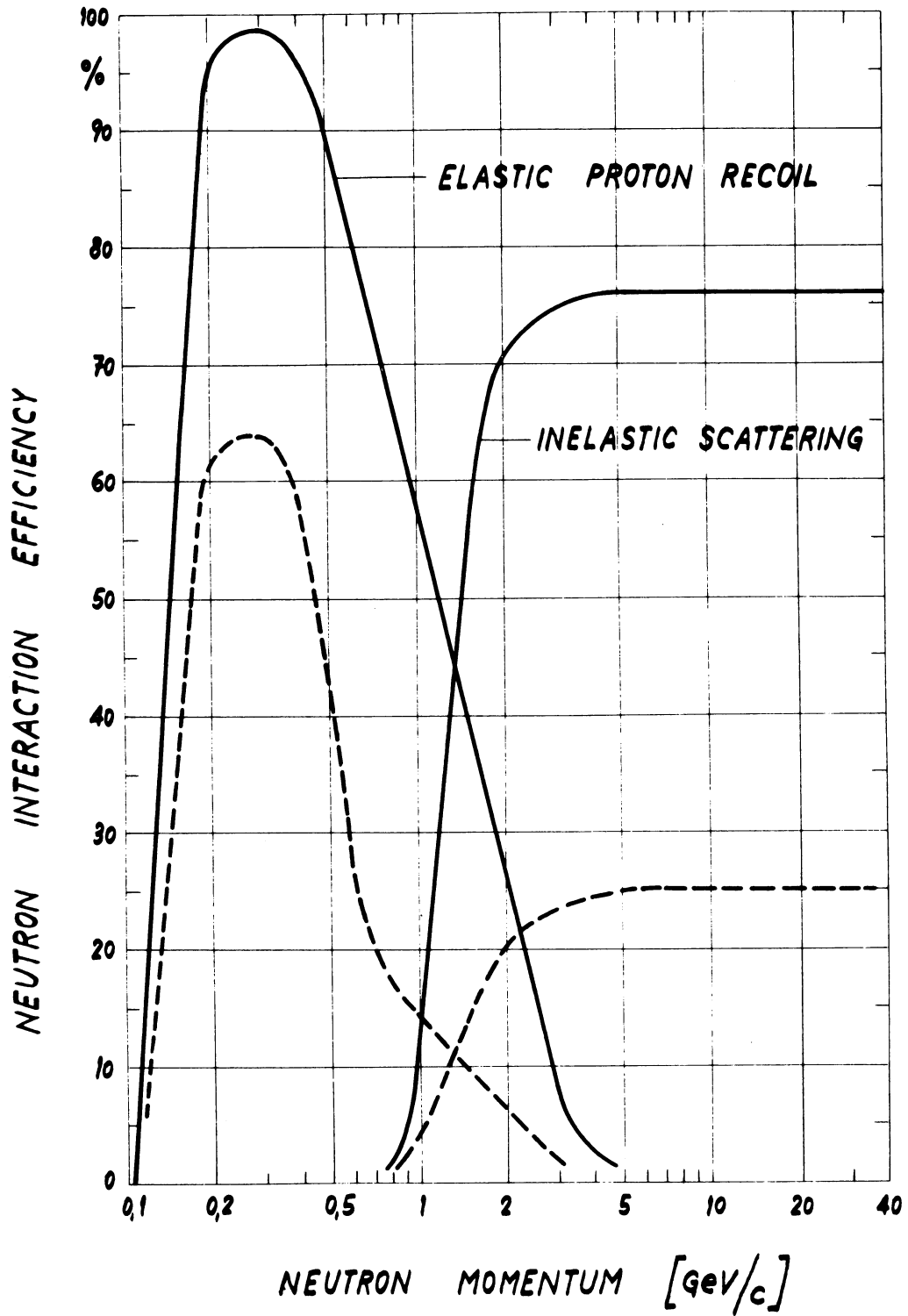


Fig. 5: Directions of π -mesons emerging from (π^- , p) reactions at 100 GeV/c primary momentum.



— 10 m LIQUID HYDROGEN
- - - 2 m LIQUID HYDROGEN

Fig. 6: Neutron interaction efficiency in liquid hydrogen

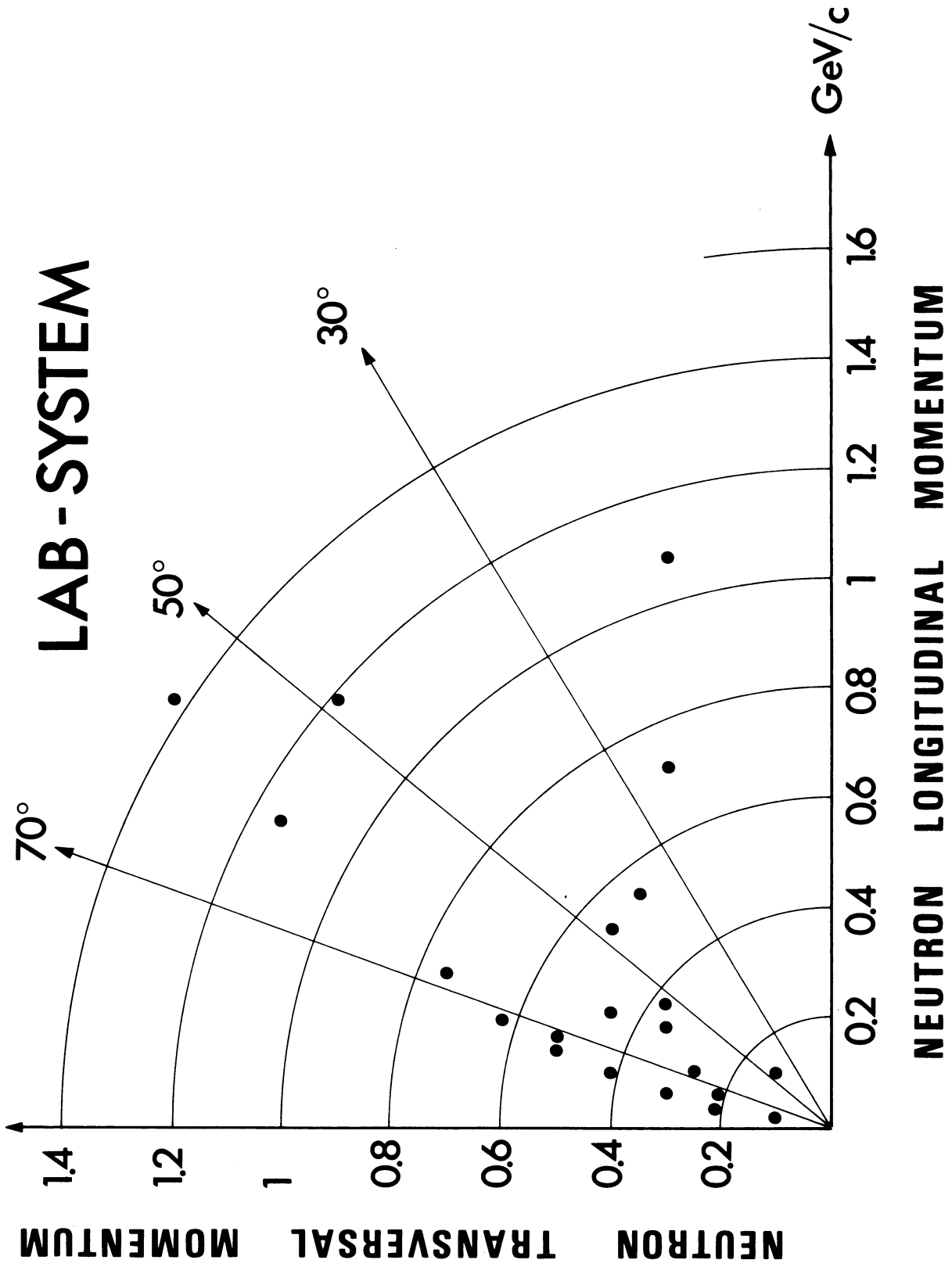


Fig. 7: Directions of neutrons emerging from (π^-, p) reactions at 100 GeV/c primary momentum